Influence of Configuration Mixing in Intermediate States on Resonant Multiphoton Ionization

E. Matthias,[a] P. Zoller,[b] D. S. Elliott, N. D. Piltch, and S. J. Smith[c]
Joint Institute for Laboratory Astrophysics, University of Colorado and National Bureau of Standards, Boulder, Colorado 80309

and

G. Leuchs
Sektion Physik der Universität München, D-8046 Garching, Federal Republic of Germany

(Received 7 March 1983)

Resonant three-photon ionization of Ba to a structureless continuum via $6snd$ Rydberg states was performed in the range $19 \leq n \leq 30$. It is shown that state mixing in the Rydberg states strongly affects the photoion and photoelectron yields as well as the angular distributions of photoelectrons. The experimental results are explained on the basis of a three-channel quantum-defect theory for the perturbed Rydberg series.

PACS numbers: 32.80.Fb, 32.80.Kf

Resonant multiphoton ionization (RMPI) contains information about the electronic structure for each of the states in the excitation-ionization sequence.[1,2] However, RMPI has hitherto only been employed to investigate the structure and decay of autoionizing states.[2,3] Here we describe the first use of RMPI to study the electronic structure of intermediate *bound* states, and we show that state mixing dramatically influences both the total ion yield and the angular distributions of photoelectrons. Although we selected Ba to demonstrate these effects, the results are of general importance for RMPI of atoms with more than one valence electron.

In Ba the $5d7d$ doubly excited configuration causes strong state mixing in the $6snd$ Rydberg states near $n = 26$.[4-8] The RMPI was chosen to proceed via these $6snd\ ^{1,3}D_2$ states. Experimentally, the $6snd$ series ($19 \leq n \leq 30$) is convenient since the yttrium-aluminum-garnet (YAlG) laser used for ionization reaches both the $6s$ and $5d$ continua of Ba^+ without exciting any autoionizing state.[9] Hence, two groups of photoelectrons are observed: *fast* ones (1.16 eV) originating from the $6s$ continuum and *slow* ones (0.46 eV) from the $5d$ continuum. The spectra in Fig. 1 were obtained by focusing the beams of two pulsed dye lasers (553.7 nm, $6s^2\ ^1S_0 \rightarrow 6s6p\ ^1P_1$ and 419–424 nm, $6s6p\ ^1P_1 \rightarrow 6snd\ ^{1,3}D_2$) and the YAlG laser along the same axis onto a beam of Ba atoms in a field-free region. Ions were collected 2 cm downstream and detected by an ion multiplier. Electrons emitted in a half angle of 12° on a perpendicular axis had a flight path of 6.5 cm before reaching the detector, which caused a 60-ns time-of-flight separation between fast and slow electrons. Typical power levels per pulse for the three successive linearly polarized laser beams were 10^2 W (553.7 nm), 5×10^3 W (419–424 nm), and 2 MW (1064 nm) in a focal diameter of of about 1 mm at the atom beam.

The influence of the $5d7d\ ^1D_2$ perturber state (in jj coupling[4] $5d_{5/2}\,7d_{3/2}$), located between $n = 26$ and 27, is obvious in the total ion yield [Fig. 1(a)] as well as in the spectra of fast [Fig. 1(b)] and slow [Fig. 1(c)] electrons. Below we outline an interpretation of the observed spectra according to the multichannel quantum-defect theory (MQDT). The simplest model assumes only the $6snd\ ^{1,3}D_2$ states and the perturber to be mixed:

$$|6snd, J=2\rangle = Z_1|6snd\ ^1D_2\rangle + Z_2|6snd\ ^3D_2\rangle + Z_3|5d_{5/2}\,7d_{3/2}, J=2\rangle .$$

The mixing coefficients Z_i follow from an MQDT analysis. In a Lu-Fano plot of the effective quantum numbers ν_{6s} (mod 1) vs ν_{5d} (mod 1), the energy levels lie on two separate branches.[4,10] The *continuous* branch contains the $6snd\ ^1D_2$ ($n \leq 25$) and $^3D_2$ ($n \geq 26$) states with ν_{6s} almost constant as a function of ν_{5d}. For these the admixture of the perturber state is small; instead there is strong singlet-triplet mixing. The $6snd\ ^3D_2$ ($n \leq 25$) and $^1D_2$ ($n \geq 26$) states, together with the $5d7d$ perturber, lie on the *broken* branch of the Lu-Fano plot. Along this branch ν_{6s} varies rapidly with ν_{5d} in the vicinity of the perturber, indicating that the $6s26d\ ^1D_2$ and $6s27d\ ^1D_2$ states contain large admixtures of the $5d7d$ configuration in addition to singlet-triplet mixing. This classification is identified in the ion spectrum in Fig. 1(a) where the continuous and broken branches are connected by dash-dotted and

dashed lines, respectively. The continuous branch terminates at $n=30$ since we did not resolve triplet states beyond this point.

Neglecting configuration interaction (CI) in the final state, the differential ionization rates from Rydberg states leaving behind a $6s$ or $5d$ core of Ba^+ are, in the usual notation,[1]

$$\frac{d\gamma_{6s}}{d\Omega} \propto \sum_{i=1,2} Z_i^2 \sum_{m_c m_s} |\langle 6s_{1/2} m_c; \vec{p} m_s | \vec{\mu}\vec{\epsilon} | 6snd\,^{1,3}D_2, M_J = 0\rangle|^2 I_{\mathrm{YAlG}}, \tag{1a}$$

$$\frac{d\gamma_{5d}}{d\Omega} \propto Z_3^2 \sum_{j=3/2}^{5/2} \sum_{m_c m_s} |\langle 5d_j m_c; \vec{p} m_s | \vec{\mu}\vec{\epsilon} | 5d7d\,^1D_2, M_J = 0\rangle|^2 I_{\mathrm{YAlG}}, \tag{1b}$$

with the assumption of orthogonal radial wave functions. The sum includes angular quantum numbers of the ion core (m_c) and spin polarization (m_s). The ionization probability to the Ba^+-($5d$) continuum is determined by the admixture of the perturber. Hence the dominant peaks in Fig. 1(c) stem from states on the broken branch of the Lu-Fano plot; the nearly constant background for $n \leq 24$ indicates the presence of non-resonant CI. In addition to the n dependence of state mixing, the radial matrix elements involved in the excitation sequence may change over the perturbed region. They are almost constant along the continuous branch (apart from an overall decrease with n) and show for the broken branch a Fano profile as a function of energy near the perturber.

The intensities in Fig. 1 can be described by rate equations since the measurements satisfy broad bandwidth conditions.[1] If W is the excitation rate of the Rydberg states and κ their spontaneous decay rate, the ionization probabilities

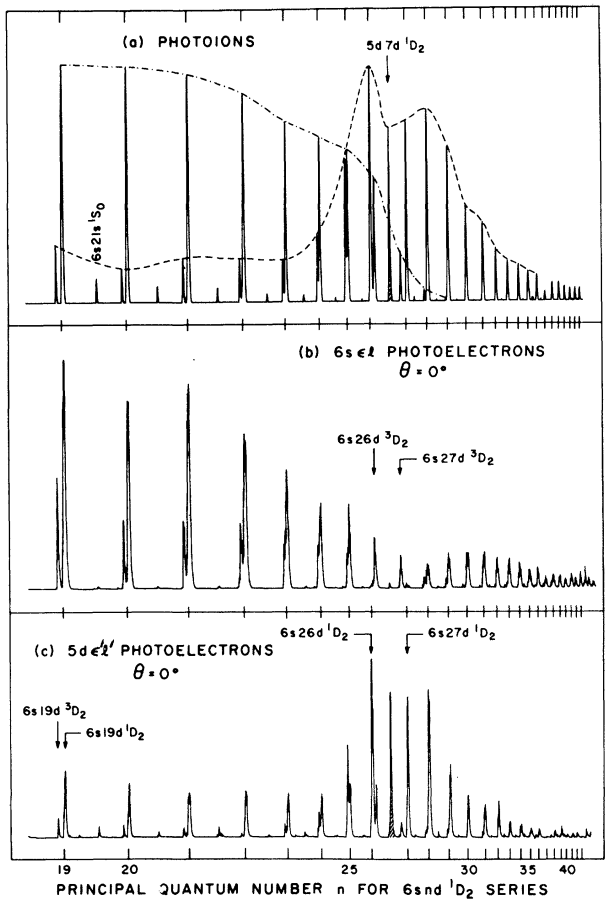

FIG. 1. (a) Total yield of photoions for resonant three-photon ionization of Ba. (b) and (c) Angle-resolved and time-gated spectra of electrons originating from the $6s$ and $5d$ continua of Ba^+.

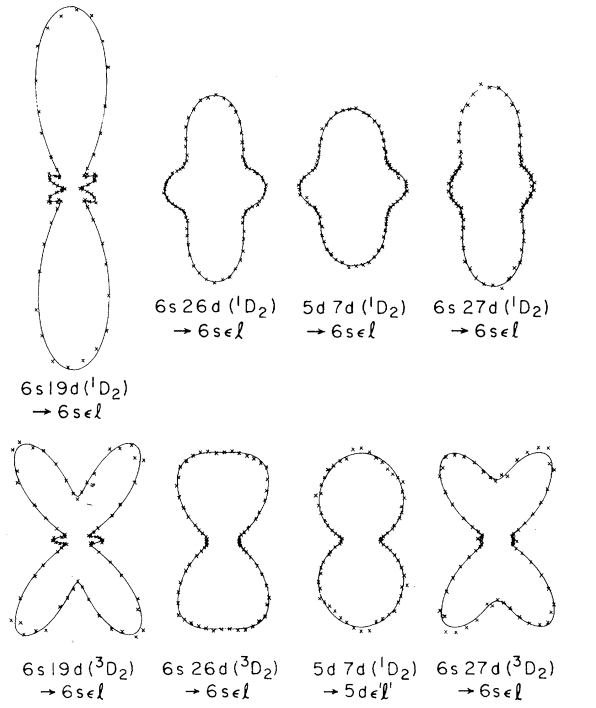

FIG. 2. Selected angular distributions of photoelectrons following RMPI of Ba. The $\theta = 0$ axis points vertically; the linear polarizations of the three laser beams were aligned parallel. The solid lines are least-squares fits.

starting from the $6s6p$ state can be written

$$\frac{d}{d\Omega}P_{6s,5d} = \frac{W}{\kappa+2W}\left[1-e^{-(\kappa+2W)T}\right]e^{-\kappa\tau}\,\frac{d(\gamma_{6s,5d})/d\Omega}{\gamma_{6s}+\gamma_{5d}+\kappa}\left\{1-\exp\left[-(\kappa+\gamma_{5d}+\gamma_{6s})T\right]\right\}. \quad (2)$$

The first three factors describe the population remaining in the Rydberg states at time τ following excitation by a laser pulse of duration T; the last two represent the branching of the ionization signal. Since the $6s6p\,^1P_1$ state couples predominantly to the singlet part of the wave function, $W \propto Z_1^2|R_{6p}^{nd}|^2 I_{\text{blue}}$. Thus, the contribution from states on the continuous branch of the Lu-Fano plot disappears near the pure[10] $6s30d\,^3D_2$ in both ion and fast-electron spectra [Figs. 1(a) and 1(b)]. Along the broken branch W reaches a maximum near the perturber state, because of an increase in the singlet admixture and a decrease in the radial matrix elements with n. The ionization signal is further enhanced by the higher ionization rate of the $7d$ electron [Eq. (1b)] compared to the Rydberg electron. In the perturbed region the ion yield is thus dominated by the Ba^+ $5d$ channel. The amplitude of the resonance in Figs. 1(a) and 1(c) is determined by the choice of laser polarization and by saturation of the ionization step. The observed double hump at $n=26$ and 28 is explained by the reduction of radiative lifetimes caused by the $5d7d$ admixture,[5] which allows Rydberg states on the broken branch to decay during the $\tau \cong 30$ ns interval between exciting and ionizing radiation. Finally, the minimum near the perturber in Fig. 1(b) is caused by the large $5d7d$ admixture which, for the broken branch, diverts most of the Rydberg state population into the $5d\epsilon' l'$ continuum.

Additional information about the coupling of the two valence electrons and the continuum wave functions can be obtained from the angular distribution of photoelectrons which from Eqs. (1) has the form[1] $W(\theta)=\sum_{l=0}^{N=3}A_{2l}P_{2l}(\cos\theta)$. Here, θ is the angle between the electron momentum and the polarization vectors of the light. The coefficients A_{2l} contain information about the structure of the states involved.[11] Using the techniques developed by Leuchs and Smith,[12] we measured angular distributions of photoelectrons originating from $6snd$ states in the range $19 \leq n \leq 30$. The experimental conditions were identical to the ones used for recording the electron spectra in Figs. 1(b) and 1(c); the polarization vectors of the laser light were rotated synchronously by half-wave plates. In Fig. 2 a few typical angular distributions illustrate the change in shape when passing from almost unperturbed $6snd$ states through the perturbed region. The angular distribution for $6s30d\,^1D_2 \rightarrow 6s\epsilon l$ has again the same appearance as the one for $6s19d\,^1D_2 \rightarrow 6s\epsilon l$.

To illustrate how to extract information from the angular distribution coefficients we will discuss A_6, which is not complicated by p-f interferences. For the normalized A_6 coefficient Eq. (1a) predicts

$$\frac{A_6}{A_0} = \frac{\frac{40}{77}\left(\frac{3}{2}Z_1^2|R_s^f|^2 - Z_2^2|R_t^f|^2\right)}{Z_1^2\left(\frac{4}{15}|R_s^p|^2+\frac{9}{35}|R_s^f|^2\right)+Z_2^2\left(\frac{1}{5}|R_t^p|^2+\frac{8}{35}|R_t^f|^2\right)}, \quad (3)$$

where $R_s^{p,f}$ and $R_t^{p,f}$ denote the radial matrix elements for singlet or triplet ionization. To calculate A_6, we assume $R_s \simeq R_t$ and find the ratio of radial matrix elements from quantum defect theory to be $|R^p|^2/|R^f|^2 \simeq 0.5$. The admixture coefficients were drawn from the MQDT analysis.[10] The result is plotted as a solid line in Fig. 3(a), together with values of A_6 obtained from the measured angular distributions and corrected for the finite solid angle. We observe overall agreement between theory and experiment. In particular, the data points for the nearly pure singlet and triplet states at $n=19$ and 30 are well reproduced by the above approximations. Deviations between experimental data and theory for $n=24$ and 25 are attributed to insufficient spectral resolution. The A_6 coefficients directly reflect the n dependence of Z_1^2 shown in Fig. 3(b). A change from singlet to triplet character leads to a change of sign for A_6 according to Eq. (3). Along the continuous branch of the Lu-Fano plot, the angular distributions consist of a superposition of pure singlet and triplet distributions. The situation is more complex for the broken branch near the perturber because the small probability for photoionization to the $6s$ continuum allows second-order effects, such as final-state CI, to become dominant. A typical angular distribution of $5d\epsilon' l'$ electrons is illustrated in Fig. 2 for $5d7d\,^1D_2$. It consists mainly of an A_2 term, characteristic of an isotropic state, because A_6

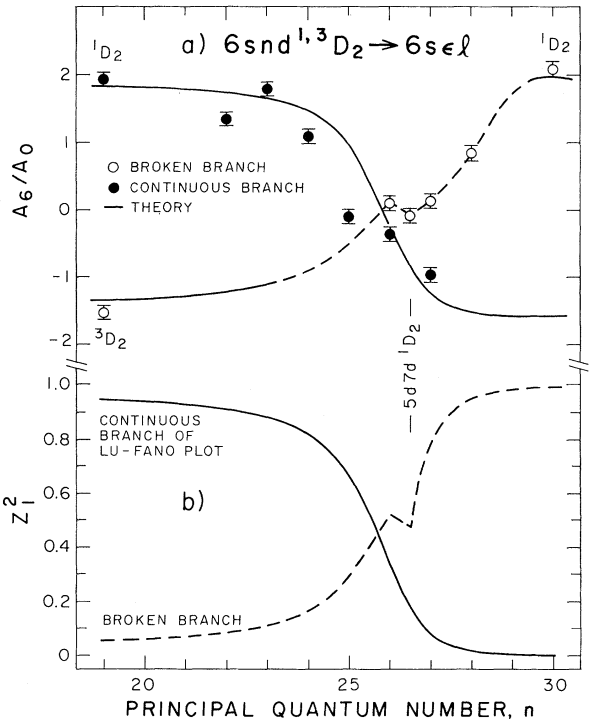

FIG. 3. (a) Experimental and theoretical angular distribution coefficients A_6/A_0. The solid line was calculated with use of Eq. (3). The theoretical model does not apply to electrons from states on the broken branch near the perturber (dashed lines). (b) Singlet admixture of $6snd\ ^{1,3}D_2$ states in Ba derived from an MQDT analysis (Ref. 10).

vanishes for a pure $5d_{5/2}7d_{3/2}$ state[4] and the A_4 term is smeared out by the angular momentum exchange between the core and the ionized electron.

In summary, we have demonstrated that for RMPI both the total ion yield and the angular distribution of photoelectrons are sensitive probes for studying the structure of *bound* excited states. In particular the angular distribution proves to be uniquely sensitive to the detailed structure of the perturbing configuration and to nonresonant CI. We anticipate that these techniques will become important for the investigation of atoms with mixed configurations and will provide new input data for improved MQDT analyses.

This work was supported in part by National Science Foundation Grants No. PHY82-00805 and No. INT-8120128, and by a grant from the Deutsche Forschungsgemeinschaft. We are grateful to J. Andru and to R. Weppner for technical contributions.

[a]Visiting Fellow. Permanent address: Freie Universität Berlin, D-1000 Berlin 33, West Germany.
[b]Visiting Fellow. Permanent address: Institute for Theoretical Physics, University of Innsbruck, 6020 Innsbruck, Austria.
[c]Staff member, Quantum Physics Division, National Bureau of Standards, Boulder, Colo. 80309.

[1]P. Lambropoulos, Adv. At. Mol. Phys. 12, 87 (1976); A. T. Georges and P. Lambropoulos, Adv. Electron. Electron Phys. 54, 191 (1980).
[2]D. Feldmann and K. H. Welge, J. Phys. B 15, 1651 (1982).
[3]J. J. Wynne and J. P. Hermann, Opt. Lett. 4, 106 (1979); M. Aymar, P. Camus, and A. El Himdy, J. Phys. B 15, L759 (1982); N. H. Tran, R. Kachru, and T. F. Gallagher, Phys. Rev. A 26, 3016 (1982); W. E. Cooke and S. A. Bhatti, Phys. Rev. A 26, 391 (1982), and references therein.
[4]M. Aymar and O. Robaux, J. Phys. B 12, 531 (1979).
[5]K. Bhatia, P. Grafström, C. Levinson, H. Lundberg, L. Nilsson, and S. Svanberg, Z. Phys. A 303, 1 (1981); M. Aymar, R.-J. Champeau, C. Delsart, and J.-C. Keller, J. Phys. B 14, 4489 (1981).
[6]P. Grafström, C. Levinson, H. Lundberg, S. Svanberg, P. Grundevik, L. Nilsson, and M. Aymar, Z. Phys. A 308, 95 (1982).
[7]M. L. Zimmerman, T. W. Ducas, M. G. Littman, and D. Kleppner, J. Phys. B 11, L11 (1978).
[8]H. Rinneberg and J. Neukammer, Phys. Rev. Lett. 49, 124 (1982); P. Grafström, J. Zhan-Kui, G. Jönsson, S. Kröll, C. Levinson, H. Lundberg, and S. Svanberg, Z. Phys. A 306, 281 (1982).
[9]R. D. Hudson, V. L. Carter, and P. A. Young, Phys. Rev. A 2, 643 (1970).
[10]H. Rinneberg and J. Neukammer, Phys. Rev. A 27, 1779 (1983).
[11]J. A. Duncanson, Jr., M. P. Strand, A. Lindgard, and R. S. Berry, Phys. Rev. Lett. 37, 987 (1976); G. Leuchs, S. J. Smith, and H. Walther, in *Laser Spectroscopy IV*, edited by H. Walther and K. W. Rothe, Springer Series in Optical Sciences Vol. 21 (Springer, Heidelberg, 1979), p. 255; J. C. Hansen, J. A. Duncanson, Jr., R.-L. Chien, and R. S. Berry, Phys. Rev. A 21, 222 (1980), and references therein.
[12]G. Leuchs, in Laser Physics, Proceedings of the Third New Zealand Summer School, edited by D. F. Walls and J. D. Harvey (to be published), and references therein.